WILEY

Large-scale physical facility and experimental dataset for the validation of urban drainage models

E. Sañudo | **L. Cea** | **J. Puertas** | **J. Naves** | **J. Anta**

Universidade da Coruña, Water and Environmental Engineering Group, Center for Technological Innovation in Construction and Civil Engineering (CITEEC), A Coruña, Spain

Correspondence
E. Sañudo, Universidade da Coruña, Water and Environmental Engineering Group, Center for Technological Innovation in Construction and Civil Engineering (CITEEC), Campus de Elviña, 15071 A Coruña, Spain.
Email: e.sanudo@udc.es

Abstract

Numerical models are currently the main tool used to simulate the effects of urban flooding. The validation of these models requires thorough and accurate observed data in order to test their performance. The current study presents a series of laboratory experiments in a large-scale urban drainage physical facility of approximately 100 m^2 that includes roofs, streets, inlets, manholes and sewers. The facility is equipped with a rainfall simulator as well as a surface runoff and pipe inflows generators. The experiments were divided in two sets. In Set 1 the surface runoff was generated exclusively by the rainfall input, while in Set 2 the rainfall simulator was used in combination with the runoff generators. In all the tests the water discharge was measured at points on the inlets, roofs, and outfall. The water depth at different locations of the facility was also measured. The experimental tests were replicated numerically using the urban drainage model Iber-SWMM. Experimental results show that, even in a relatively small catchment the peaks in the hydrographs generated at each element of the facility during intermittent rainfalls are significantly attenuated at the catchment outlet. The agreement between the experimental and numerical results show that there are some differences in the hydrographs generated at each element, but that these differences compensate each other and disappear at the outfall. The results generated provide the research community with a thorough and high-resolution dataset obtained under controlled laboratory conditions in a large-scale urban drainage facility, something which has not previously been available.

KEYWORDS
experimental dataset, physical model, rainfall simulator, rainfall-runoff experiments, urban drainage, urban hydrology

1 | INTRODUCTION

Extreme rain events, which are becoming more and more frequent, test the capacity and operation of urban drainage systems. In many cases the drainage networks of cities are obsolete, deficient, or have low levels of retrofit and maintenance that can lead to human and material losses as a result of urban flooding and environmental pollution (Cea & Costabile, 2022). In addition, new urban developments and new impervious areas add extra runoff volumes to existing systems that must be managed and evacuated, adding further stress to the drainage network.

During rainfall, the overland flow is two-dimensional and is conditioned by the complexity of the urban configuration and by its interaction with the drainage network. Understanding and simulating these

complex flows is essential in assessing flood risk and sewer performance, and in proposing mitigation actions. Currently, urban drainage software are able to simulate two-dimensional surface flow and its interaction with the sewer network in an integrated way thanks to our current understanding of urban hydrology processes, significant advances in computational performance, and the development of high-resolution data acquisition technologies. These software, known as 2D/1D dual urban drainage models, solve two-dimensional shallow water equations (SWE) with a fully distributed rainfall-runoff transformation approach on the surface, while solving one-dimensional Saint-Venant equations in the sewer network. A wide range of commercial 2D/1D urban drainage software is available, such as Info works (Bertrand et al., 2022), MIKE (Haghighatafshar et al., 2018) and Bentley (Ramos et al., 2017). Despite these recent developments, free software has yet to be used extensively in real projects, remaining largely in the research sphere (Fraga et al., 2017; Yin et al., 2020; Chang et al., 2021) or enjoying only limited distribution. In general, all 2D/1D software shares the same structure: A 2D overland flow engine, a 1D sewer flow engine, and a core that synchronizes both engines and exchanges information between them. Meanwhile the 2D engine is usually self-developed software, and many 2D/1D urban drainage models use the open-source engine of the Storm Water Management Model to solve the in-sewer processes (Leandro & Martins, 2016; Barreiro et al., 2022).

The reliability and performance of urban drainage models must be validated using observed data in order to ensure that the numerical solution adequately represents reality. The availability of observed data is usually very limited due to the cost and complex set-ups required to acquire it, both in field and laboratory campaigns. Datasets obtained in field campaigns are typically used to calibrate the model parameters in real urban basins, but usually introduce measurement errors such as uncertainties in the acquisition system or in the sensor calibration processes (Fraga et al., 2016). On the other hand, the use of experimental data obtained in laboratory facilities is more suitable for assessing the performance of numerical models, since tests are carried out under strictly controlled conditions, and hence there is far lower uncertainty in terms of the input and observed data (Naves et al., 2019; Addison-Atkinson et al., 2023). For this reason, in recent years a number of studies using urban drainage laboratory facilities have been conducted to better understand the relevant processes on urban hydrology and the hydrodynamics of urban flooding (Mignot et al., 2019). Several of these studies focused on the influence of street layouts and the presence of infrastructures on the flooding processes (Dong et al., 2021; Naves et al., 2020; Naves et al., 2021), including the bidirectional flow exchange between the surface and the sewer network under non-surcharge and surcharge conditions (Fraga et al., 2017; Rubinato et al., 2017), while others have analysed the hydraulic performance of specific urban drainage components such as inlets (Russo et al., 2021), manholes (Rubinato et al., 2022) or roofs (Sañudo et al., 2022).

Many of these experiments were carried out on scale models of real urban street layouts, either on simplified geometries (Cea, Garrido, Puertas, Jácome, et al., 2010) (Cea, Garrido, & Puertas, 2010;

Mignot et al., 2020), or without considering some parts of the drainage system (e.g., the roofs of buildings), or considering drainage elements in an isolated way (Rubinato et al., 2018). In addition, in most cases the water input was generated by an upstream flow, with only a few studies using rainfall generators (Naves et al., 2021; Al Mamoon et al., 2019).

The current research presents a set of experimental tests carried out in a new large-scale urban drainage physical model, and aims to study rainfall-runoff processes in an integrated way at near-real scale, including roofs, streets, manholes, inlets, and sewers. Considering all the elements on the same facility allows for a holistic study of their operation and enables the evaluation of each element's contribution to the downstream discharge point. Understanding these contributions provides the basis for studies in urban areas where simplifications are required, or high-quality data are not available. The facility represents a section of an urban neighbourhood environment and is equipped with a high precision rainfall simulator, two surface runoff generators, and two pipe inflows generators. The facility setup makes it possible to control the rainfall and flow inputs and to measure hydraulic variables at custom points. All the information necessary to replicate the experimental tests is provided with high spatial resolution. In addition, numerical validation using the Iber-SWMM software was carried out based on the presented dataset. Iber-SWMM (Sañudo et al., 2020) is a 2D/1D hydraulic model that combines the freely distributed hydraulic model Iber (Bladé et al., 2014) with SWMM engine via Dynamic Link Libraries (DLL), with the aim of providing a freely distributed resource for the scientific community and practitioners.

The goals of this research are: (i) to describe a new large-scale laboratory urban drainage facility; (ii) to present and assess a first experimental dataset obtained at this facility; (iii) to present a digital twin of the facility based on the 2D/1D model Iber-SWMM and replicate numerically the experimental tests. All the experimental data and results are available at the open-access repository Zenodo (Sañudo et al., 2023).

2 | MATERIALS AND METHODS

2.1 | Laboratory set-up

2.1.1 | Description of the urban drainage facility

The large-scale urban drainage facility (hereafter the block) is located in the Hydraulics Laboratory of the Centre of Technological Innovation in Construction and Civil Engineering (CITEEC) at the University of A Coruña (Spain). The facility, which measures of 100 m^2, consists of three main parts (Figure 1): a rainfall simulator, a street surface (including roofs and pavements), and a sewer network linked to it. The rainfall simulator can generate constant intensities of 30, 50, and 80 mm/h with high spatial uniformity. The street surface (Figure 2) consists of a T-intersection of two 2.5 m wide concrete roads and four blocks of buildings. The roadway and the building blocks are separated by a concrete tiled pavement, 30 cm wide, and a 6 cm high
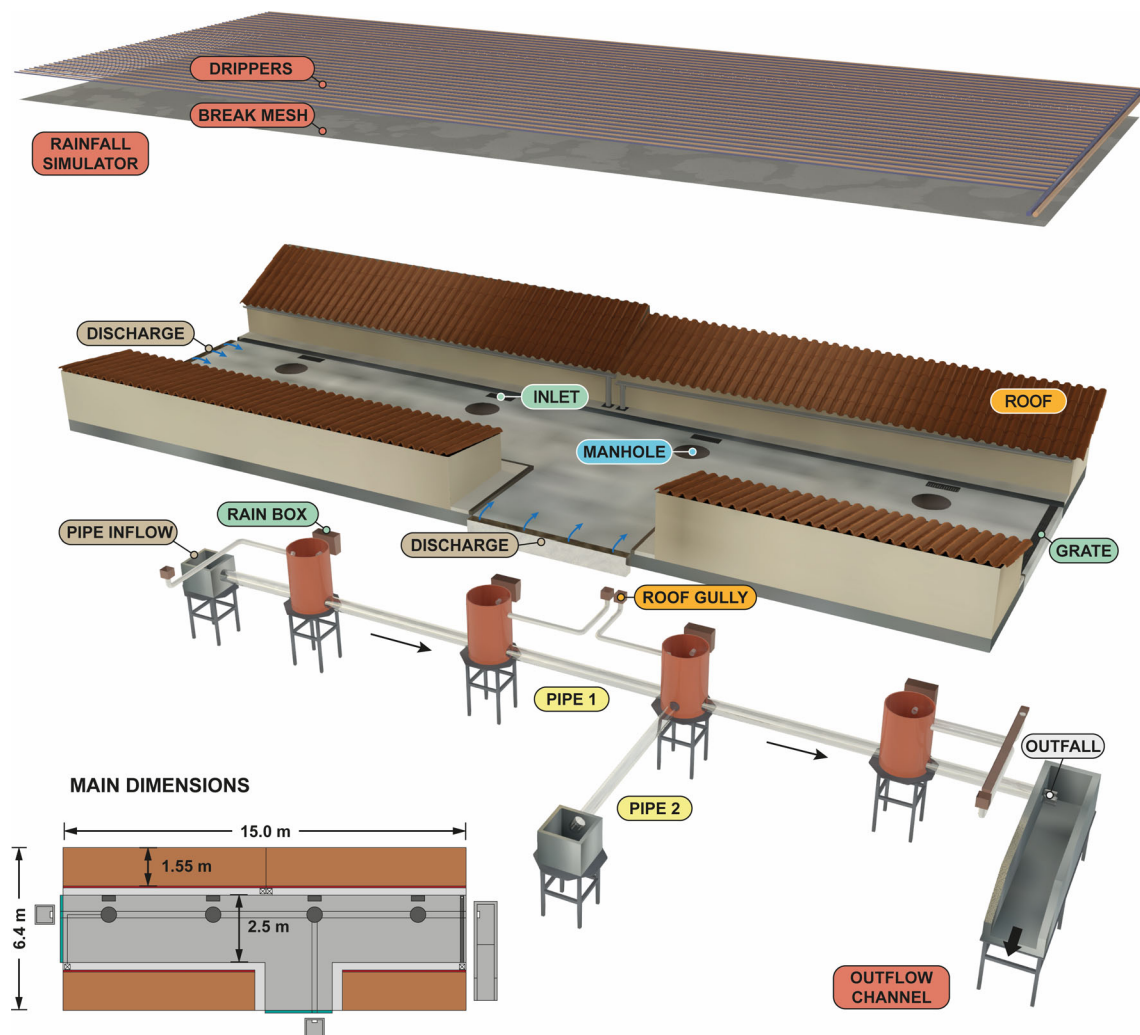
FIGURE 1 Conceptual scheme of the urban drainage facility.

concrete curb. The roadway and pavements have a longitudinal slope of 1% and a transversal slope of 2%, respectively. The buildings have ceramic tiled roofs and semi-circular gutters. More information on the rainfall generator, the characterization of the rainfall, and the configuration of the roofs is given in Sañudo et al. (2022). The facility is fully equipped with ultrasonic depth sensors and flowmeters. In addition, it has a pumping system that allows the generation of two controlled surface runoff flows from the upstream boundaries to the surface of each road (SD) and two controlled inflows at the beginning of each pipe (PI). The sewer network (Figure 2) consists of four manholes (MH), two pipelines (PL), two boundary inflow gullies (PI) on the pipelines upstream boundaries, and an outfall (O) that spills all the water of the facility into an open channel equipped with a triangular weir. The main pipeline, with an inner diameter of 240 mm, covers the longitudinal dimension of the facility and connects the upstream inflow PI1, the manholes MH1, MH2, MH3, and MH4, and the outfall (O1). Additionally, a transversal pipeline, of an inner diameter of 194 mm, joins the inflow PI2 with the manhole MH3. Both pipelines intersect at MH3 and are made of methacrylate. The manholes have an outer

diameter of 800 mm and a thickness of 20 mm and are not hermetically sealed so water can enter through these into the sewer system. Their surface diameter is 580 mm, and they are closed with an iron cover. The surface and the sewer system are linked through 4 rectangular inlets of 0.5 × 0.2 m and a downstream transversal grate of 2.5 × 0.13 m that covers the width of the roadway. Each inlet has a drain box of 0.46 × 0.16 × 0.38 m and is directly connected to the nearest manhole by a 90 mm PVC pipe. Neither the drain box nor the pipe connection limits the inlet flow capacity. Similarly, the grate has its own drain box of the same length and width, and is 8 cm deep. The grate is directly connected to MH4.

Roof runoff is conveyed through the gutters to the downspouts, which discharge into 4 gully pots, one for each roof. The roof gully pots are connected to their associated manhole by 90 mm PVC pipes. Thus, ROOF1 is connected to MH1, ROOF2 to MH4, ROOF3 to MH3, and ROOF4 to MH2 (Figures 1 and 2). The origin of the local coordinate system is established at the geometric centre of the facility and at the floor level of the laboratory. All the coordinates and georeferenced data are referenced to this local system.
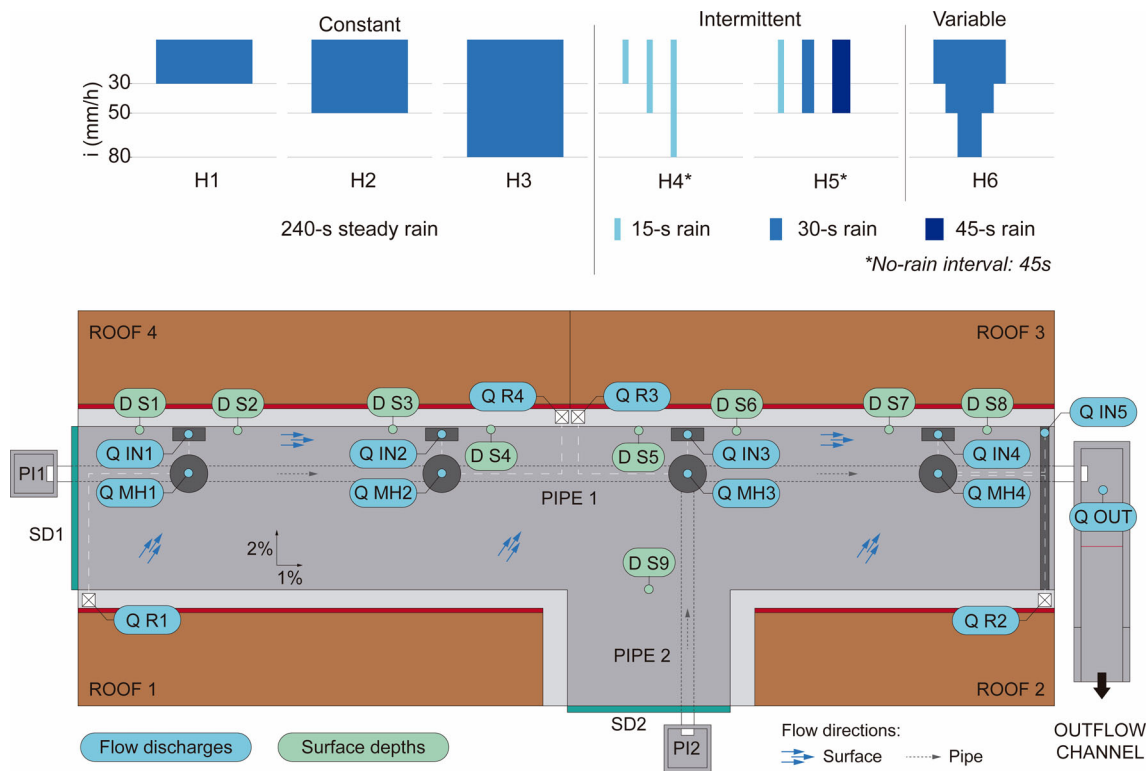
FIGURE 2 Hyetographs generated in each test and location of the flow and depth measurement points.

2.1.2 | Experimental procedure

The aim of the experiments was to achieve an accurate characterization of surface and in-sewer runoffs by measuring the discharges on roofs, inlets, and at the outlet of the whole facility. In addition, depths at different surface points were also measured. The tests were divided into two sets: Set 1, in which all the runoff is generated by the rainfall simulator; and Set 2, in which the runoff is generated by the rainfall simulator plus both runoff generators. Pipe inflow generators were not used in these experiments, and hence the sewer base flow was not considered. Wet antecedent conditions were considered in all the experiments due to the long period required by the facility to become completely dry. To prevent residual flows from previous test, a 30 min time gap was left between tests.

Six different hyetographs with varying intensities and durations were generated in the experiments (Figure 4). Hyetographs H1, H2 and H3 are defined by a constant rainfall intensity of 30, 50, and 80 mm/h respectively, sustained over a period of 4 min. Hyetographs H4 and H5 represent intermittent rainfall consisting of 15, 30, and 45 s rain intervals with 45 s of no rain between them. Hyetograph H6 is characterized by a quasitriangular symmetric pattern, with six rain periods of 30 s each and with a maximum intensity of 80 mm/h.

First, Set 1 was carried out by performing 6 tests, one for each hyetograph, using only the rainfall simulator. Then, for Set 2, tests on Set 1 were repeated adding a constant flow of 1 L/s in each of the runoff generators. The runoff flows were steady during the tests. Table 1 shows the configurations for the 12 tests performed.

The discharge was measured at the outlet of each roof, at each inlet, at the downstream grate, and at the outlet of the facility.

Generally, the manholes in sewer networks are correctly sealed to prevent odours and surface runoff intakes, but this is not the case in stormwater networks. Since manholes covers are usually not hermetically sealed in real storms sewer networks, it was decided not to seal them in the facility either. Therefore, some flow entered through their boundaries from the surface to the manhole. For this reason, the discharge that entered through the manholes into the sewer network was also measured. In addition to the discharge measurements, water depths were measured at 9 points on the surface, 8 of these 0.5 m upstream and 0.5 m downstream from each of the four inlets and 6 cm from the curb. Another depth measurement was obtained at the intersection of the streets.

2.1.3 | LiDAR acquisition and drainage network mapping

A good quality Digital Elevation Model (DEM) is key to addressing 2D/1D urban drainage models (Allitt, 2009) and to obtaining reliable results. The methodology adopted in the present study to obtain a high-resolution 3D surface model of the whole facility is described in (Sañudo et al., 2022), and uses an Intel® RealSense™ LiDAR Camera L515 sensor. The final product was a DEM with a cell resolution of 5 mm (Figure 3). In addition, the dimensions of manholes, inlets and grates were measured with a graded meter. Finally, break lines were obtained to force the elements of the computational mesh along them, especially in high slope changes such as curbs.

A mapping of the drainage network was also carried out. The x and y coordinates were obtained by triangulation from at least two

reference points. The z coordinate was obtained by measuring the distance between the measurement point and a horizontal laser plane established as a reference.
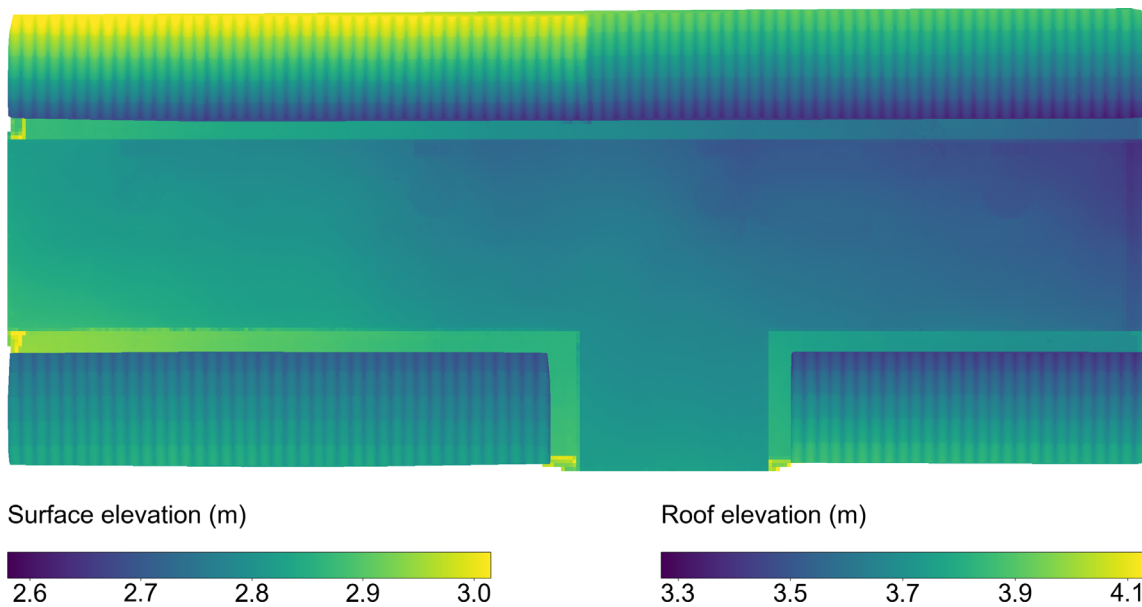
2.1.4 | Flow and depth measurements

First, roof discharges were measured following the methodology used in Sañudo et al. (2022) where a detailed analysis of rainfall-runoff transformation processes in roofs is presented. Roof discharge was estimated by measuring the rate of variation of the water level with respect to time in a square tank located at the gutter outlet.
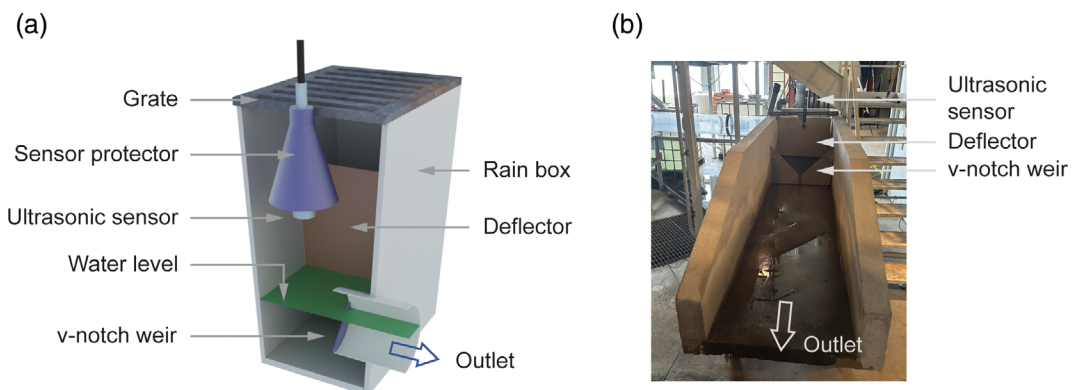
Next, the flow captured at each inlet was measured using plastic pre-calibrated v-notch weirs located at the outlet of each drain box (Figure 4a). An ultrasonic depth sensor was located below each inlet grate to measure the depth in the drain box. A deflector was carefully installed inside the drain box to avoid high frequency oscillations of the free surface that would introduce excessive noise in the registered signal. It should be noted that this method of measuring the inlet discharge is non-intrusive. Similarly, the outlet discharge of the whole facility was estimated from the water level variation over a metallic triangular weir located at the channel outfall (Figure 4b). Manholes and grate discharges were obtained only under steady state conditions, due to the complexity of installing a sensor.

**TABLE 1** Summary of the hydraulic test configurations.

Test	Set 1						Set 2					
	T1	T2	T3	T4	T5	T6	T7	T8	T9	T10	T11	T12
Rainfall	H1	H2	H3	H4	H5	H6	H1	H2	H3	H4	H5	H6
Runoff	✖	✖	✖	✖	✖	✖	✓	✓	✓	✓	✓	✓

Surface elevation (m)

2.6   2.7   2.8   2.9   3.0

Roof elevation (m)

3.3   3.5   3.7   3.9   4.1

FIGURE 3 Digital Elevation Model of the roofs obtained using LiDAR.

(a)

Grate
Sensor protector
Ultrasonic sensor
Water level
v-notch weir

Rain box
Deflector

Outlet

(b)

Ultrasonic sensor
Deflector
v-notch weir

Outlet

FIGURE 4 Setup for the flow discharge measurement at the inlet (a) and at the outlet channel (b) using an ultrasonic depth sensor.
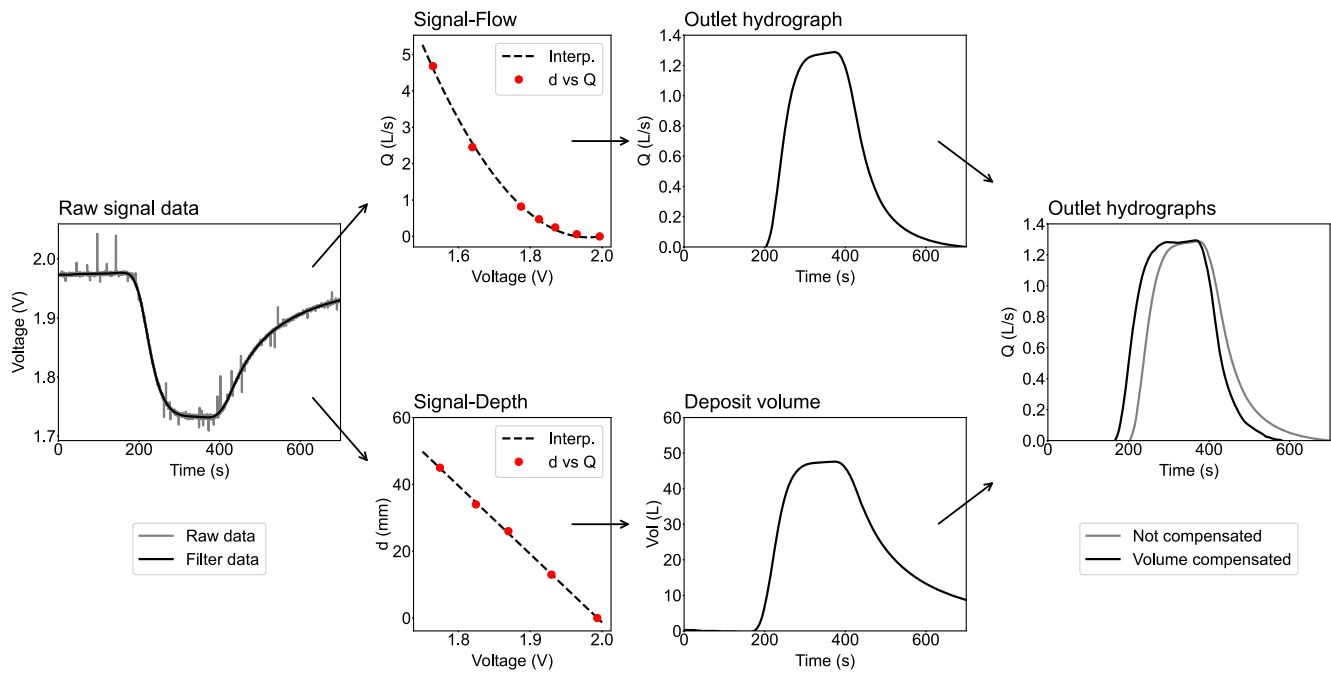
FIGURE 5 Methodology of data processing for obtaining the outlet hydrograph at the outfall of the sewer network. The raw signal data is converted to flow and volume (depth × area) using pre-calibrated curves and rating curves. The compensated outlet hydrograph is obtained by adding the flow storage to the measured hydrograph.

For measuring distance, ultrasonic pre-calibrated sensors (UB500-18GM75-I-V15, Pepperl + Fuchs, Germany) with an output resolution of 0.13 mm were used. The sampling frequency was set to 5 Hz. A low-pass filter was applied to the raw signal to eliminate outliers and reduce the noise. For all tests, recording began 120 s prior to the start of the rain.

The replicability of the tests is mainly conditioned by the ability of the rainfall simulator to generate identical rainfall intensities between runs. The replicability and the consistency of the rainfall intensities generated was verified in (Sañudo et al., 2022), so the methodology was considered to be fully repeatable. In addition, each test of Table 1 was performed twice. The comparison of the two runs showed a very high agreement for all tests, for example, less than 0.004 L/s for steady flows in tests T1, T2, and T3 was obtained, which guarantees the total replicability of the methodology. It must be noted that with this measurement setup the flows measured in the inlets and in the channel are not exactly the same as those actually entering through the inlets or exiting through the sewer outfall. This is the case because the rain boxes and the outlet channel store a volume of water that attenuates, thus delaying the measured hydrograph. Consequently, a volume compensation based on the water balance in the rain boxes and in the channel was carried out to obtain the actual hydrographs using the Equation (1):

$$\frac{\partial h}{\partial t} = \frac{(Q_{in} - Q_{out})}{A} \qquad (1)$$

where $\frac{\partial h}{\partial t}$ is the depth variation at the rain box or outflow channel, Q_{in} and Q_{out} are the flows that enter or exit on them, and A is the drain box inner area or outflow channel area. As an example, the volume compensation methodology of the outlet channel is shown in Figure 5. Thus, the flow storage on the outflow channel is added to the outflow measured to obtain the sewer outfall discharge. Same methodology was applied to the inlet inflows.

2.2 | Urban drainage software

2.2.1 | Framework of Iber-SWMM

Iber-SWMM (Sañudo et al., 2020) is a freely distributed 1D/2D dual drainage model which combines the 2D overland flow model of Iber (Bladé et al., 2014) and the 1D sewer network model SWMM (Rossman, 2015). The model considers the main urban hydrological and hydraulic processes during a rainfall event. All surface processes, such as rainfall-runoff transformation and surface hydraulics, are computed with the hydraulics module of Iber, whereas SWMM is used to compute the flow in the sewer network. The model implements a bidirectional exchange of water between the surface and the sewer network. Therefore, when the sewer system is not surcharged the water enters to the network through the inlets, while if it is surcharged the flooding can overflow to the surface through the manholes.

2.2.2 | Inlets and manholes

Inlets and manholes are the main link between the surface and the sewer system. Inlets are the main entrance of water to the network

under non-surcharged conditions, while manholes act as water sources to the streets under surcharged conditions. However, under non-surcharged conditions, if the manhole covers are not sealed, water can also enter through these into the sewer system. Iber-SWMM considers this possibility by including formulations, which consider surface water inflow through manholes. For this purpose, the model computes the discharge capacity of inlets and manholes $(Q_{2D/1D})$ by means of the widely used weir (2) and orifice (3) formulae:

$$Q_{2D/1D\,weir} = c_w \cdot W \cdot h^{\frac{3}{2}} \tag{2}$$

$$Q_{2D/1D\,orifice} = c_o \cdot A \cdot h^{\frac{1}{2}} \tag{3}$$

where c_w and c_o are the weir and orifice coefficients, respectively, W and A is the perimeter and area of the element (inlet or manhole), respectively, h is the hydraulic head, and g is the acceleration of gravity.

Although some authors also consider the inclusion of the rain boxes (Dong et al., 2021), others dismiss their effect in the propagation of runoff (Martins et al., 2018). Iber-SWMM does not contemplate the modelling of rain boxes, due to the low impact that these have in real applications. For manhole capacity formulae, the same formulae are implemented as for the inlets.

2.2.3 | Roofs

(Sañudo et al., 2022) showed that the use of semi-distributed models is the most efficient approach to compute rainfall-runoff transformation in the roofs of buildings and to evaluate their outlet hydrographs. Therefore, Iber-SWMM models the roofs as individual subcatchments,

and implements the non-linear reservoir equation to compute the hydrograph generated by the rainfall over roofs. The non-linear reservoir model represents the subcatchment as a shallow storage (Rossman & Huber, 2016), in which the output hydrograph Q (m^3/s) is controlled by the Manning equation (4):

$$Q = \frac{1}{n} \cdot W \cdot S^{\frac{1}{2}} \cdot (d - d_s)^{\frac{5}{3}} \tag{4}$$

where n ($s/m^{1/3}$) is the Manning coefficient of the roof, W (m) is the subcatchment width, S (m/m) is the subcatchment slope, d(m) is the water depth, and d_s (m) is the storage depth that fixes the virtual reservoir capacity and sets the initial abstraction. Outflow only occurs when the depth exceeds the depression storage and the slope is different from zero.

Roof systems in urban settings can be directly connected to the sewer network or unconnected to it. In Iber-SWMM, the user can define whether the roof is connected to the sewer network, unconnected, or if a percentage of the discharge is sent to the nearest manhole, to the street, or even infiltrates into the ground.

2.2.4 | Model setup

The street domain was discretised using a triangular unstructured mesh with an average element size of 0.05 m. On the other hand, the domain of the roofs was discretized using a structured mesh with an element size of 0.2 m, since these are computed with a lumped approach and hence no mesh resolution is needed. The numerical mesh of the model has a total of 40 000 elements. Currently this extremely high resolution is not feasible in practical applications because it would lead to very high computational times (Ramsauer et al., 2021).
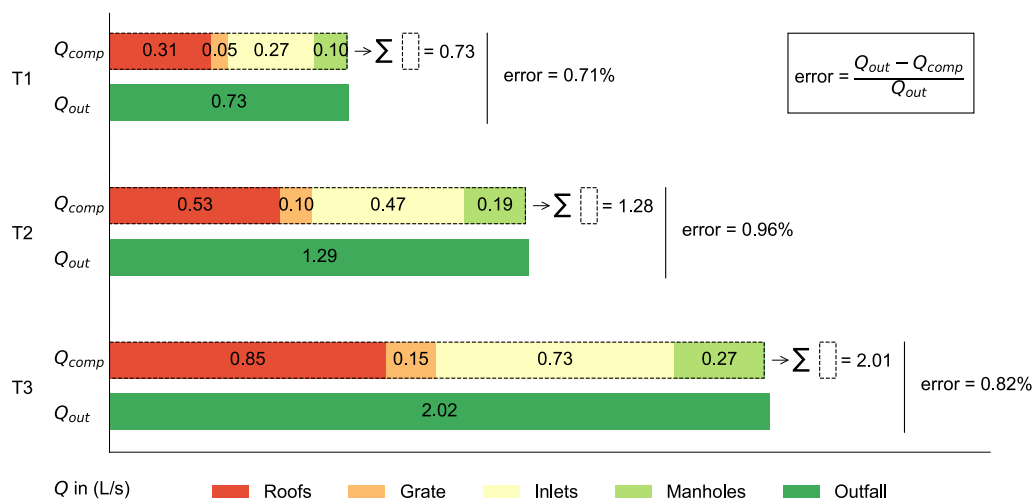
FIGURE 6 Experimental mass balance computed as the error between the addition of the discharge measured at the roofs, inlets, grate, and manhole (Q_{comp}) and the discharge at the outfall (Q_{out}) under steady conditions.

The Manning coefficient was set to 0.016 on the street surface (Naves et al., 2019), 0.025 on the roofs, and 0.008 in the pipes, since these latter are made of plastic and are completely clean. It is highlighted that no initial abstraction was defined on any surface, since the experiments were performed under wet antecedent conditions. Experimental tests were carried out one after the other leaving
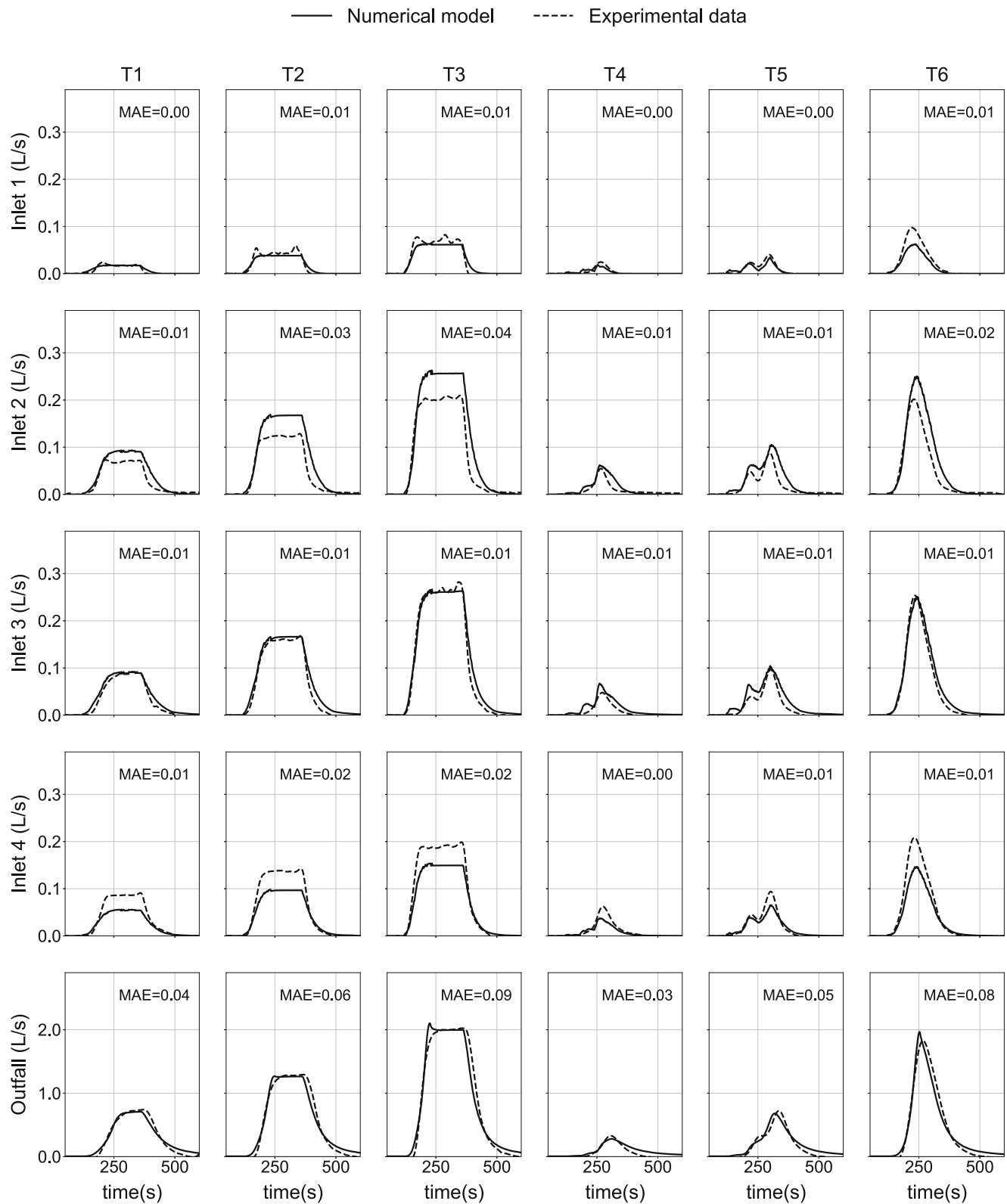
FIGURE 7 Comparison of the experimental and numerical discharges obtained for tests using only the rainfall simulator (Set 1).

only shorts periods of time between them to avoid residual flows from one test to another. This implies that small surface irregularities were filled at the beginning of each experiment. To guarantee that both the experimental and numerical tests start from the same initial conditions the numerical model included an initial rainy warm-up period to fill the potential surface irregularities, followed by a dry period to let the residual flows to drain. The numerical simulations were carried out using a wet-dry threshold of 0.1 mm and the decoupled hydrological discretization (DHD) scheme suitable for surface runoff computations in urban catchments and small-scale rural basins (Cea & Bladé, 2015). The Dynamic Wave routing model with a 1 s routing step was used in the SWMM module.

The rain maps used were those obtained through the rain characterization performed in (Sañudo et al., 2022). The rain maps were introduced as rasters with average rain intensities of 30.3, 54.2, 85.0 mm/h for the three rainfalls that the simulator can generate. For simplicity, we will refer to these intensities as 30, 50, and 80 mm/h.

3 | RESULTS AND DISCUSSION

This section presents the experimental results for the tests of Set 1 and Set 2. The presentation and discussion of the experimental results is accompanied by numerical results, and the fitting between the experimental results and numerical simulations is also addressed. Results on roofs were presented in Sañudo et al. (2022) so are not included in the present study.

3.1 | Experimental discharges

In order to characterize the relative contribution of each element (roofs, inlets, manholes, and grate) to the outlet hydrograph, as well as a first-level control of the experiments, an experimental mass balance was calculated from the measured hydrographs (Figure 6). The difference between the total volume of water captured by the roofs, inlets, grate, and manholes and the spilled by the sewer outfall under steady

flow conditions was less than 1% in tests T1, T2, T3. This implies that there are no uncontrolled flows in the experiments.

The manholes captured approximately 14% of the total precipitation. Although this percentage might depend on the way in which the manhole covers are placed, it is not a negligible amount, so it is important take it into account in the numerical modelling of the experiments. Inlets captured 36% of the total precipitation. Visual observations showed that the discharge capacity of the inlets was not exceeded in the experiments, and thus all the water flow arriving at the inlet was captured. The downstream grate collected the runoff that was not collected by the inlets and manholes, which represented approximately 7% of the total precipitation. Approximately 42% of the total volume originated from the roof's hydrographs. This value is directly proportional to their surface area, which underlines the importance of including a detail definition of roofs for modelling purposes, especially in highly consolidated urban areas with a high percentages of buildings. These relative contributions of each element of the system remained practically the same for all the tests shown in Figure 6, with differences lower than 1% for all the tests.

### 3.2 | Inlets, manholes and outfall discharges

Figure 7 shows the flow rates measured in tests T1 to T6 (Set 1) on the inlets and on the outfall, as well as the results obtained with the

TABLE 2 Experimental and numerical volume contribution percentages for each type of element.

|		Inlets	Grate	Manholes	Roofs
T1	Num.	36.6%	6.6%	13.6%	43.2%
	Exp.	36.4%	7.3%	13.5%	42.8%
T2	Num.	38.3%	6.6%	13.2%	41.9%
	Exp.	36.6%	7.4%	14.6%	41.3%
T3	Num.	37.6%	7.0%	12.9%	42.4%
	Exp.	36.5%	7.6%	13.7%	42.3%
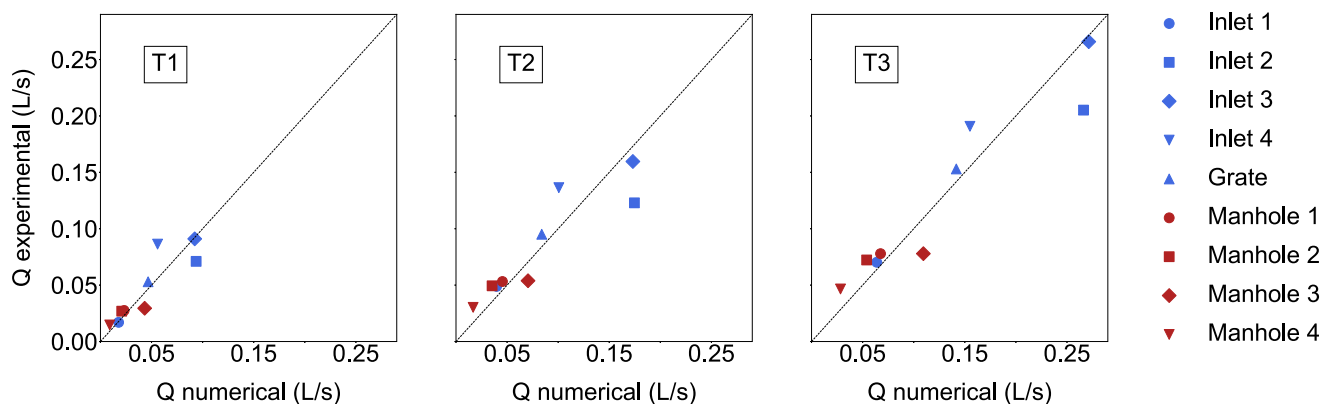
FIGURE 8 Comparison of numerical and experimental steady flow rates captured by inlets and manholes. Results are shown for the three constant rainfall intensities: T1 = 30, T2 = 50, and T3 = 80 mm/h.
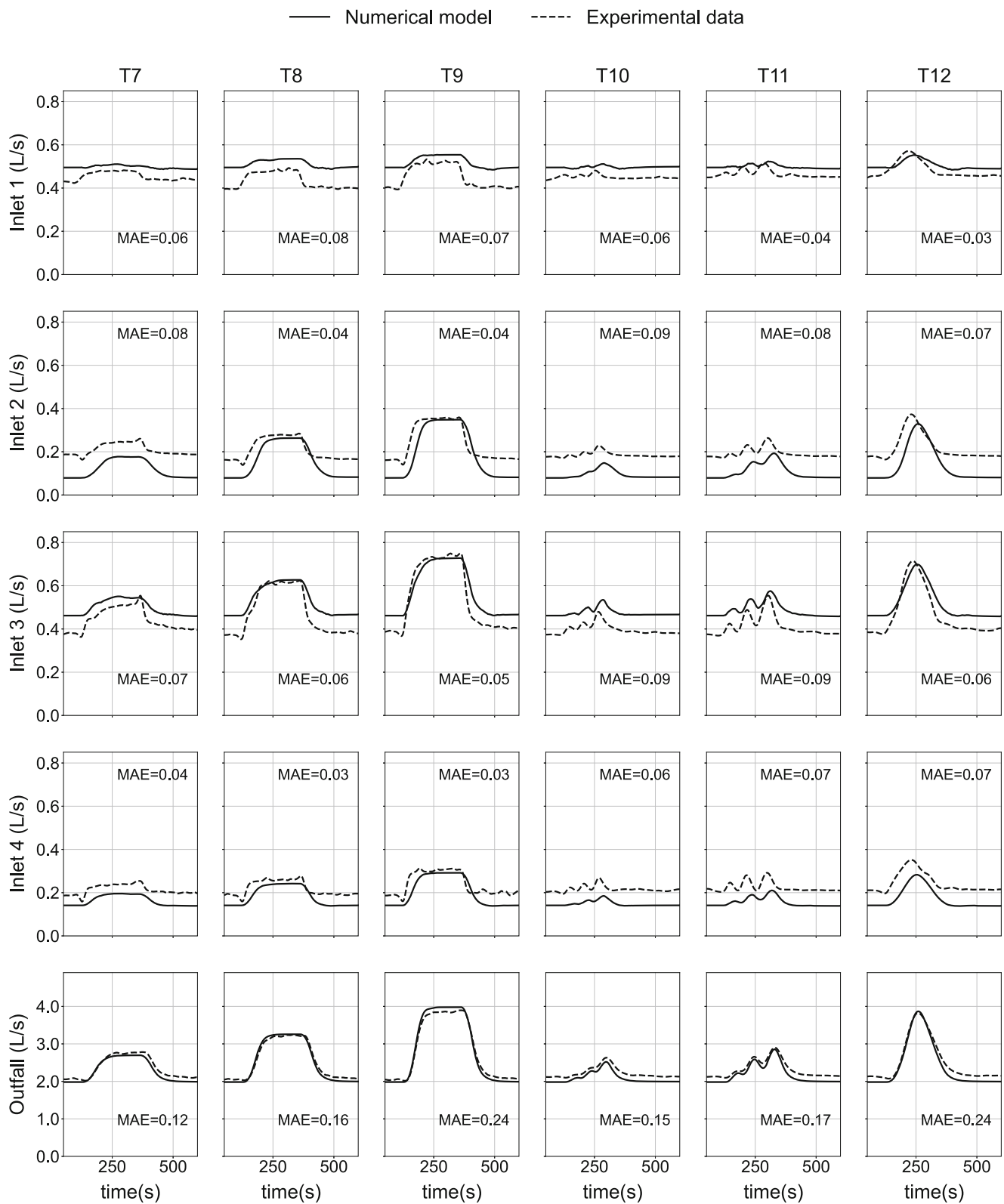
FIGURE 9 Comparison of the experimental and numerical discharges obtained for tests using only the rainfall simulator plus the runoff generators (Set 2).

numerical model Iber-SWMM. Note that Inlet 1 has a small upstream contribution area, while Inlet 3 captures most of the runoff arriving from the intersection. Thus, Inlet 1 and Inlet 3 capture the lowest and

the highest flow rates, respectively, the computed and measured hydrographs being proportional to their contribution areas. The agreement between the experimental and numerical results was quantified
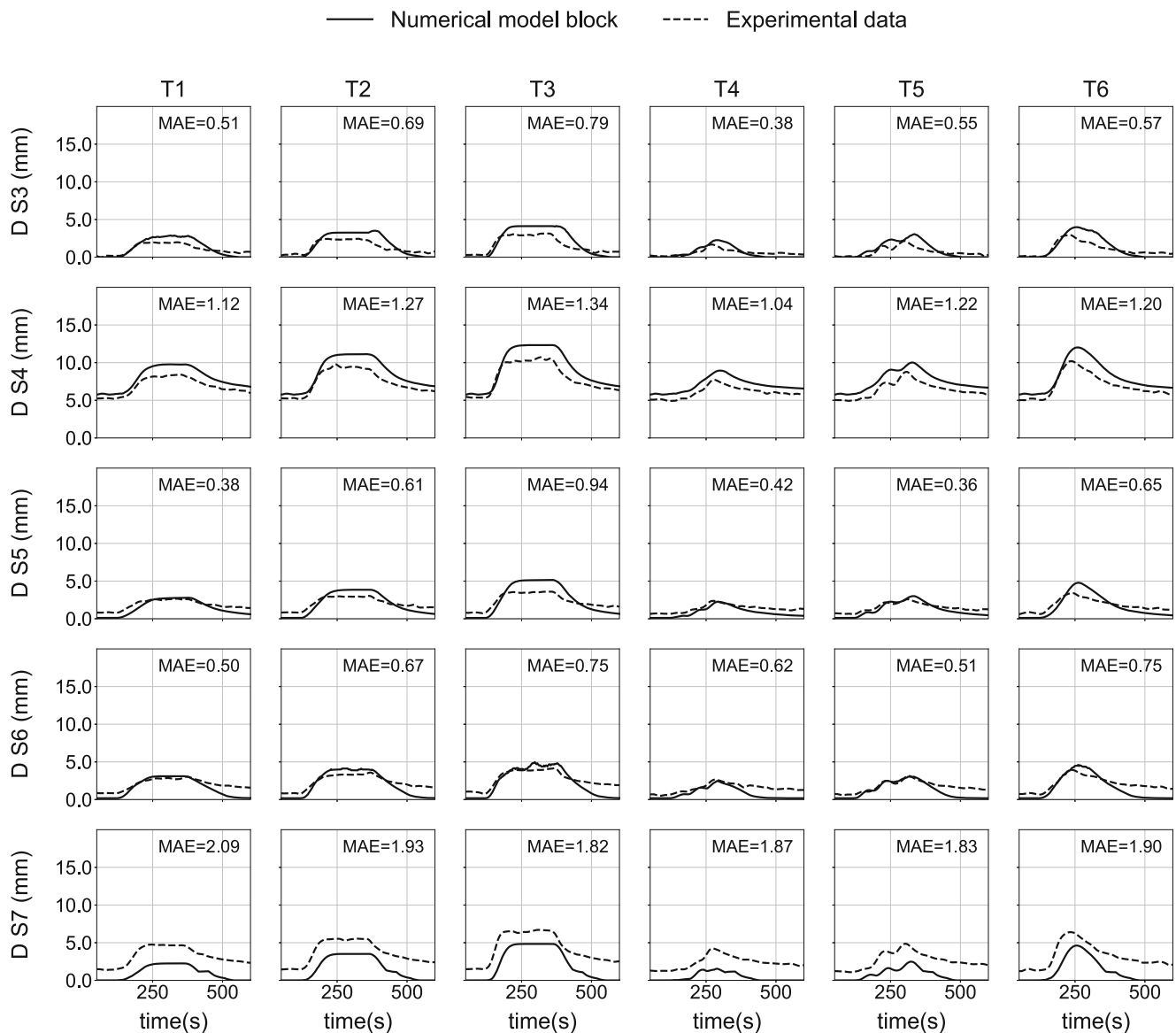
FIGURE 10 Comparison of the experimental and numerical depths obtained for tests using only the rainfall simulator (Set 1).

with the Nash-Sutcliffe Efficiency coefficient (NSE) and with the Mean Absolute Error (MAE). There are some differences between the observed and computed hydrographs in some inlets. This is due to small features in the topography that slightly change the flow path of the surface runoff. Nevertheless, the observed and computed outfall hydrographs show a very good fit, with an average NSE and MAE (considering the six experimental tests) of 0.93 and 0.05 L/s, respectively. This means that the numerical-experimental differences in the computed hydrographs at each inlet compensate each other when the flow converges at the facility outfall. Thus, in practice, for model calibration and validation purposes the use of measurements at locations that receive water from several inlets is recommended, in order to avoid the effect of small topographic features that cannot be resolved with the numerical model.

As noted in section 2, the inflow through the manhole covers was measured under steady flow conditions. In the numerical model, the discharge capacity of manholes was manually calibrated, since

the manholes were partially sealed. The agreement between the experimental and numerical discharges that enter through the manholes is shown in Figure 8. The results show a good correlation, with an R-squared greater than 0.9 for the three tests.

Table 2 shows the volume of water drained by the different elements of the facility, estimated from the experiments and from the numerical model. The numerical-experimental agreement is very good, with the largest volume contribution being from the roofs, followed by the inlets.

The results of Set 2, in which the surface runoff is generated by the rainfall simulator and by the runoff generators, are shown in Figure 9. For this set of experiments, the water drained through the manholes was not measured, so the numerical configuration of the discharge capacity used in Set 1 was also used in Set 2 (i.e., no calibration). Again, the experimental-numerical fit is far better at the facility outfall than at the inlets. The initial discharge of the hydrographs in this case is not zero, due to the steady flow introduced by the runoff
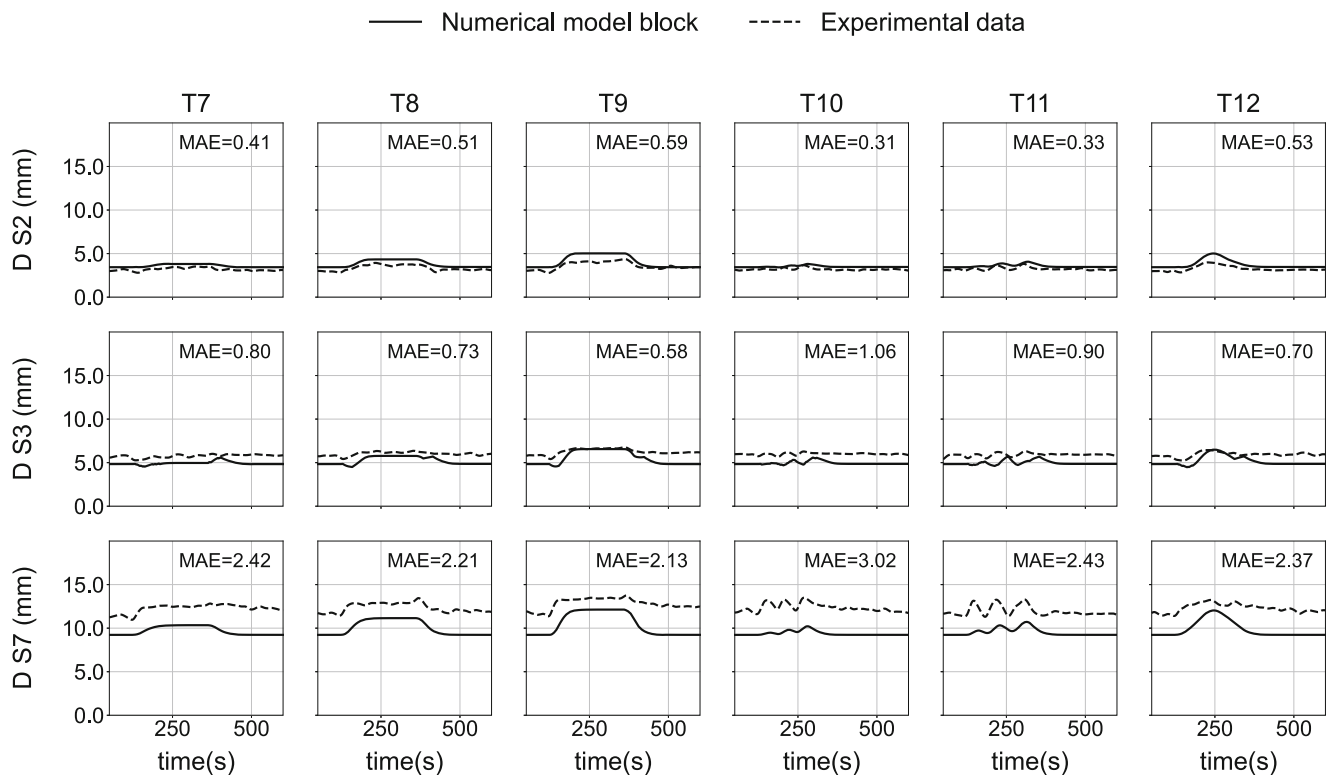
FIGURE 11   Comparison of the experimental and numerical depths obtained for tests using only the rainfall simulator plus the runoff generators (Set 2).

generators. The numerical model is not able to reproduce precisely how this initial steady runoff is distributed through each individual inlet. On the other hand, the prediction is good at the facility outfall, which means that the model preserves mass continuity through the whole facility. Despite these differences, in general terms the shape of the numerical hydrographs shows a satisfactory agreement with the experiments. At the facility outfall, the agreement between the numerical and experimental hydrographs is very good in all the tests, once again showing that the errors in the computed hydrographs at each inlet compensate each other at the global outfall.

3.3 | Water depths

The measured and modelled water depths at the street surface locations DS3, DS4, DS5, DS6 and DS7 are shown in Figure 10 for the experiments of Set 1. The average MAE is approximately 0.5 mm at DS3, DS5, and DS6, 1.2 mm at DS4, and 1.9 mm at DS7. These differences are very small considering that the magnitude of the water depth in the experiments is of the order of 1 cm. For instance, the water depth at locations DS1, DS2, DS8 and DS9 is less than 2 mm due to their small contribution area. As already mentioned in section 0, even if the topography was measured with a very high accuracy and spatial resolution, small irregularities in the topography can lead to certain discrepancies in the experimental-numerical agreement of the water depth at some locations. The fit at location DS7 is

especially bad since the numerical model does not correctly represent the initial depth at the beginning of the experiment. Notice that the initial water depth is not zero at locations DS4, DS5, and DS6, due to the fact that the tests were carried out under antecedent wet conditions, which left residual ponds, especially near the curb. This is especially notable at DS4, where the shape of the topography generates a large pond of 5 mm depth located downstream from Inlet 2.

Figure 11 shows the water depths obtained in Set 2 at locations DS2, DS3 and DS7. In this case, the initial water depth is not zero at all the locations due to the steady flow generated by the runoff generators. The numerical-experimental agreement at control points DS2 and DS3 shows a good fit, with an average MAE of 0.6 mm and a correct representation of the shape of the depth time series. On the other hand, the results at control point DS7 present a poor fit due to the poor agreement of the initial depth condition that implies an offset, however the shape of the time series is reproduced correctly. This offset appears due to small features in the surface of the experimental facility that are not properly reproduced in the numerical topography, and that slightly change the surface flow paths. The offset is similar to the observed at DS7 in the Set 1 for the same reason (Figure 10).

4 | CONCLUSIONS

A large-scale urban drainage physical model equipped with a rainfall simulator has been presented, together with an experimental dataset

that includes measurements of water depths and discharges at the outlet of several components of the facility (roofs, inlets, manholes and grate). The dataset also provides a high-resolution characterization of the rainfall input and the geometry of the facility. This material can be used for the development, validation, and assessment of 2D/1D dual urban drainage models.

The numerical modelling of the experiments shows relatively poor fits to the observations when compared at specific locations of the facility, since those measurements and results are strongly influenced by irregularities in the topography or by the spatial variability of rainfall. Nevertheless, the shape of the hydrographs measured at the inlets and at the outlet of roofs during intermittent rainfalls is substantially attenuated at the outfall of the sewer system, and thus the numerical-experimental agreement is significantly improved at the global outlet of the facility. The good fit obtained at the system outlet justifies that modelling urban processes at element scale can be a good decision when no calibration is possible, and the input data is of high quality and high resolution.

The measurements show that the surface runoff that enters the sewer network through the (not-sealed) manholes is not negligible and should therefore be taken into consideration when seeking to reproduce the experiments in detail. For this facility, the relative contribution of each element was 42% for the roofs, 36% for the inlets, 14% for the manholes, and 7% for the downstream grate.

To date, no databases are available that include a detailed and controlled experimental characterization of the rainfall-runoff generation in the different elements of a large-scale urban drainage facility. Thus, the results presented here are a significant contribution to the urban drainage community. The dataset is available in the open-access repository Zenodo (Sañudo et al., 2023).

The authors consider that future work should be focused on a better understanding of the sensitivity of the numerical results to variables as the mesh size, spatial resolution of the topography, or the location of the inlets. The validation of the modelling approach under surcharged conditions in order to assess manhole flooding should also be addressed in future works.

ACKNOWLEDGEMENTS

CONFLICT OF INTEREST STATEMENT

The authors declare no conflicts of interest.

DATA AVAILABILITY STATEMENT

The data that support the findings of this study are openly available in ZENODO at https://doi.org/10.5281/ZENODO.7941067.

ORCID

E. Sañudo https://orcid.org/0000-0003-3200-114X
L. Cea https://orcid.org/0000-0002-3920-0478
J. Puertas https://orcid.org/0000-0001-6502-0799
J. Naves https://orcid.org/0000-0001-9031-756X
J. Anta https://orcid.org/0000-0003-2002-0618

REFERENCES

Addison-Atkinson, W., Chen, A. S., Rubinato, M., Memon, F. A., & Shucksmith, J. D. (2023). Quantifying flood model accuracy under varying surface complexities. *Journal of Hydrology*, *620*, 129511. https://doi.org/10.1016/J.JHYDROL.2023.129511

Al Mamoon, A., Jahan, S., He, X., Joergensen, N. E., & Rahman, A. (2019). First flush analysis using a rainfall simulator on a micro catchment in an arid climate. *Science of the Total Environment*, *693*, 133552. https://doi.org/10.1016/j.scitotenv.2019.07.358

Allitt, R. (2009). *Coupled 1D – 2D modelling in urban areas* (pp. 1–20). WaPUG USER NOTE 40.

Barreiro, J., Santos, F., Ferreira, F., Neves, R., & Matos, J. S. (2022). Development of a 1D/2D urban flood model using the open-source models SWMM and MOHID land. *Sustainability*, *15*(1), 707. https://doi.org/10.3390/SU15010707

Bertrand, N., Abily, M., Lambert, M., & Delestre, O. (2022). Benefit of coupling 1D-2D model over an urban area to assess runoff during a Storm event. In P. Gourbesville, G. Caignaert (Eds.), *Advances in hydroinformatics. Springer Water* (pp. 315–328). Springer. https://doi.org/10.1007/978-981-19-1600-7_20

Bladé, E., Cea, L., Corestein, G., Escolano, E., Puertas, J., Vázquez-Cendón, E., Dolz, J., & Coll, A. (2014). Iber: herramienta de simulación numérica del flujo en ríos. *Revista Internacional de Metodos Numericos Para Calculo y Diseno En Ingenieria*, *30*(1), 1–10. https://doi.org/10.1016/j.rimni.2012.07.004

Cea, L., & Bladé, E. (2015). A simple and efficient unstructured finite volume scheme for solving the shallow water equations in overland flow applications. *Journal of the American Water Resources Association*, *5*(3), 2. https://doi.org/10.1111/j.1752-1688.1969.tb04897.x

Cea, L., & Costabile, P. (2022). Flood risk in urban areas: Modelling, Management and adaptation to climate change. A review. *Hydrology*, *9*(3), 50. https://doi.org/10.3390/hydrology9030050

Cea, L., Garrido, M., & Puertas, J. (2010). Experimental validation of two-dimensional depth-averaged models for forecasting rainfall–runoff from precipitation data in urban areas. *Journal of Hydrology*, *382*(1–4), 88–102. https://doi.org/10.1016/J.JHYDROL.2009.12.020

Cea, L., Garrido, M., Puertas, J., Jácome, A., Del Río, H., & Suárez, J. (2010). Overland flow computations in urban and industrial catchments from direct precipitation data using a two-dimensional shallow water model. *Water Science and Technology*, *62*(9), 1998–2008. https://doi.org/10.2166/WST.2010.746

Chang, T. J., Yu, H. L., Wang, C. H., & Chen, A. S. (2021). Overland-gully-sewer (2D-1D-1D) urban inundation modeling based on cellular automata framework. *Journal of Hydrology*, *603*, 127001. https://doi.org/10.1016/J.JHYDROL.2021.127001

Dong, B., Xia, J., Zhou, M., Deng, S., Ahmadian, R., & Falconer, R. A. (2021). Experimental and numerical model studies on flash flood inundation

processes over a typical urban street. *Advances in Water Resources*, 147, 103824. https://doi.org/10.1016/j.advwatres.2020.103824

Fraga, I., Cea, L., & Puertas, J. (2017). Validation of a 1D-2D dual drainage model under unsteady part-full and surcharged sewer conditions. *Urban Water Journal*, 14(1), 74–84. https://doi.org/10.1080/1573062X.2015.1057180

Fraga, I., Cea, L., Puertas, J., Suarez, J., Jimenez, V., & Jacome, A. (2016). Global sensitivity and GLUE-based uncertainty analysis of a 2D-1D dual urban drainage model. *Journal of Hydrologic Engineering*, 21(5), 04016004. https://doi.org/10.1061/(ASCE)HE.1943-5584.0001335

Haghighatafshar, S., Nordlöf, B., Roldin, M., Gustafsson, L. G., la Cour Jansen, J., & Jönsson, K. (2018). Efficiency of blue-green stormwater retrofits for flood mitigation – Conclusions drawn from a case study in Malmö, Sweden. *Journal of Environmental Management*, 207, 60–69. https://doi.org/10.1016/J.JENVMAN.2017.11.018

Leandro, J., & Martins, R. (2016). A methodology for linking 2D overland flow models with the sewer network model SWMM 5.1 based on dynamic link libraries. *Water Science and Technology*, 73(12), 3017–3026. https://doi.org/10.2166/wst.2016.171

Martins, R., Rubinato, M., Kesserwani, G., Leandro, J., Djordjević, S., & Shucksmith, J. D. (2018). On the characteristics of velocities fields in the vicinity of manhole inlet grates during flood events. *Water Resources Research*, 54(9), 6408–6422. https://doi.org/10.1029/2018WR022782

Mignot, E., Camusson, L., & Riviere, N. (2020). Measuring the flow intrusion towards building areas during urban floods: Impact of the obstacles located in the streets and on the facade. *Journal of Hydrology*, 583, 124607. https://doi.org/10.1016/J.JHYDROL.2020.124607

Mignot, E., Li, X., & Dewals, B. (2019). Experimental modelling of urban flooding: A review. *Journal of Hydrology*, 568, 334–342. https://doi.org/10.1016/J.JHYDROL.2018.11.001

Naves, J., Anta, J., Puertas, J., Regueiro-Picallo, M., & Suárez, J. (2019). Using a 2D shallow water model to assess large-scale particle image velocimetry (LSPIV) and structure from motion (SfM) techniques in a street-scale urban drainage physical model. *Journal of Hydrology*, 575(May), 54–65. https://doi.org/10.1016/j.jhydrol.2019.05.003

Naves, J., García, J. T., Puertas, J., & Anta, J. (2021). Assessing different imaging velocimetry techniques to measure shallow runoff velocities during rain events using an urban drainage physical model. *Hydrology and Earth System Sciences*, 25(2), 885–900. https://doi.org/10.5194/hess-25-885-2021

Naves, J., Rieckermann, J., Cea, L., Puertas, J., & Anta, J. (2020). Global and local sensitivity analysis to improve the understanding of physically-based urban wash-off models from high-resolution laboratory experiments. *Science of the Total Environment*, 709, 136152. https://doi.org/10.1016/j.scitotenv.2019.136152

Ramos, H. M., Pérez-Sánchez, M., Franco, A. B., & López-Jiménez, P. A. (2017). Urban floods adaptation and sustainable drainage measures. *Fluids*, 2(4), 61. https://doi.org/10.3390/FLUIDS2040061

Ramsauer, S., Leandro, J., & Lin, Q. (2021). Inclusion of narrow flow paths between buildings in coarser grids for urban flood modeling: Virtual surface links. *Water*, 13(19), 1–20. https://doi.org/10.3390/w13192629

Rossman, L. A. (2015). STORM WATER MANAGEMENT MODEL USER'S MANUAL Version 5.1. EPA/600/R-14/413b, National Risk Management Laboratory Office of Research and Development. United States Environmental Protection Agency, Cincinnati, Ohio., September, 352.

Rossman, L. A., & Huber, W. C. (2016). Storm water Management model reference Manual volume I – Hydrology (revised) (EPA/600/R-15/162A). (p. 231). Office of Research and Development. U.S. Environmental Protection Agency. www2.epa.gov/water-research

Rubinato, M., Helms, L., Vanderlinden, M., Hart, J., & Martins, R. (2022). Flow exchange, energy losses and pollutant transport in a surcharging manhole linked to street profiles. *Journal of Hydrology*, 604, 127201. https://doi.org/10.1016/j.jhydrol.2021.127201

Rubinato, M., Martins, R., Kesserwani, G., Leandro, J., Djordjević, S., & Shucksmith, J. (2017). Experimental calibration and validation of sewer/surface flow exchange equations in steady and unsteady flow conditions. *Journal of Hydrology*, 552, 421–432. https://doi.org/10.1016/j.jhydrol.2017.06.024

Rubinato, M., Martins, R., & Shucksmith, J. D. (2018). Quantification of energy losses at a surcharging manhole. *Urban Water Journal*, 15(3), 234–241. https://doi.org/10.1080/1573062X.2018.1424217/SUPPL_FILE/NURW_A_1424217_SM7141.PDF

Russo, B., Valentín, M. G., & Tellez-álvarez, J. (2021). The relevance of grated inlets within surface drainage systems in the field of urban flood resilience. A review of several experimental and numerical simulation approaches. *Sustainability*, 13(13), 7189. https://doi.org/10.3390/su13137189

Sañudo, E., Cea, L., & Puertas, J. (2020). Modelling pluvial flooding in urban areas coupling the models Iber and SWMM. *Water*, 12(9), 2647. https://doi.org/10.3390/w12092647

Sañudo, E., Cea, L., & Puertas, J. (2022). Comparison of three different numerical implementations to model rainfall-runoff transformation on roofs. *Hydrological Processes*, 36(5), e14588. https://doi.org/10.1002/hyp.14588

Sañudo, E., Cea, L., Puertas, J., Naves, J., & Anta, J. (2023). Experimental Dataset on a Large-Scale Urban Drainage Physical Facility. https://doi.org/10.5281/ZENODO.7941067

Yin, D., Evans, B., Wang, Q., Chen, Z., Jia, H., Chen, A. S., Fu, G., Ahmad, S., & Leng, L. (2020). Integrated 1D and 2D model for better assessing runoff quantity control of low impact development facilities on community scale. *Science of the Total Environment*, 720, 137630. https://doi.org/10.1016/j.scitotenv.2020.137630